

stke.sciencemag.org/cgi/content/full/13/615/eaay7315/DC1

Supplementary Materials for  
**Spatial and temporal alterations in protein structure by EGF  
regulate cryptic cysteine oxidation**

Jessica B. Behring, Sjoerd van der Post, Arshag D. Mooradian, Matthew J. Egan, Maxwell I. Zimmerman,  
Jenna L. Clements, Gregory R. Bowman, Jason M. Held\*

\*Corresponding author. Email: [jheld@wustl.edu](mailto:jheld@wustl.edu)

Published 21 January 2020, *Sci. Signal.* **13**, eaay7315 (2020)  
DOI: 10.1126/scisignal.aay7315

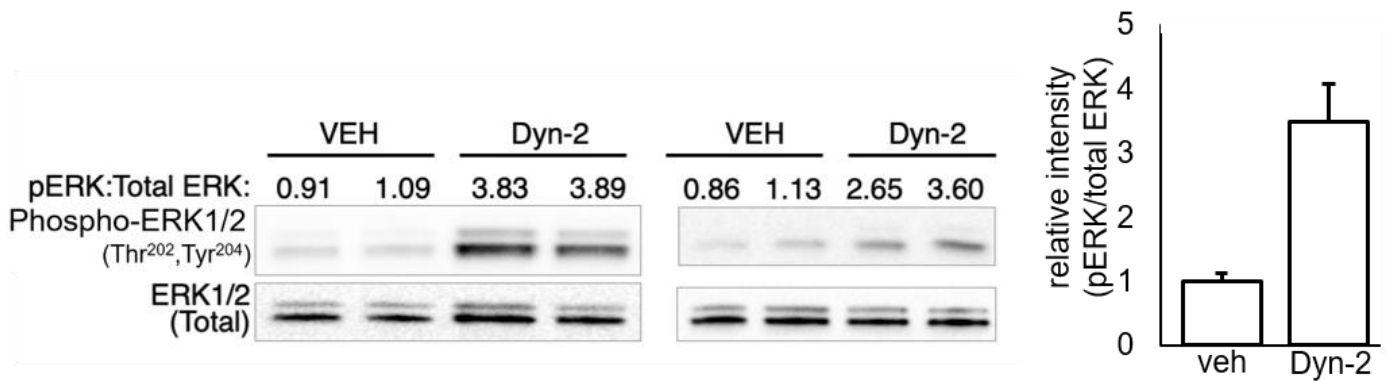
**The PDF file includes:**

Fig. S1. In situ DYn-2 treatment alters EGFR-dependent ERK phosphorylation.  
Fig. S2. OxRAC method validation and controls.  
Fig. S3. Redox regulation of protein kinases and phosphatases.  
Fig. S4. EGF-dependent redox regulation of AAA ATPases and small GTPases.  
Fig. S5. Biochemical properties of the identified oxidized cysteine residues.  
Legends for data files S1 to S4

**Other Supplementary Material for this manuscript includes the following:**

(available at [stke.sciencemag.org/cgi/content/full/13/615/eaay7315/DC1](http://stke.sciencemag.org/cgi/content/full/13/615/eaay7315/DC1))

Data file S1 (Microsoft Excel format). Table of all cysteine residues detected, their LC-MS information and intensities, and redox regulation.  
Data file S2 (Microsoft Excel format). PANTHER and Reactome annotations for peptides (and associated genes) assigned to each temporal cluster.  
Data file S3 (Microsoft Excel format). IPA canonical pathways enriched at each time point.  
Data file S4 (Microsoft Excel format). Representation of Pfam domain and family annotations within the OxRAC dataset.



**Fig. S1. In situ DYN-2 treatment alters EGFR-dependent ERK phosphorylation.** Serum starved A431 cells were prepared as for OxRAC, but the cells were treated with DYN-2 or vehicle for 1 hour as in (24) (5mM dyn-2 in DMSO, 1 hr). Western blot to phospho-Thr<sup>202</sup>/Tyr<sup>204</sup> ERK and total ERK. DYN-2 significantly increases levels of phospho-ERK ( $p = 0.002$ ,  $N=4$  biological replicates, t-test, error bars represent standard deviation).

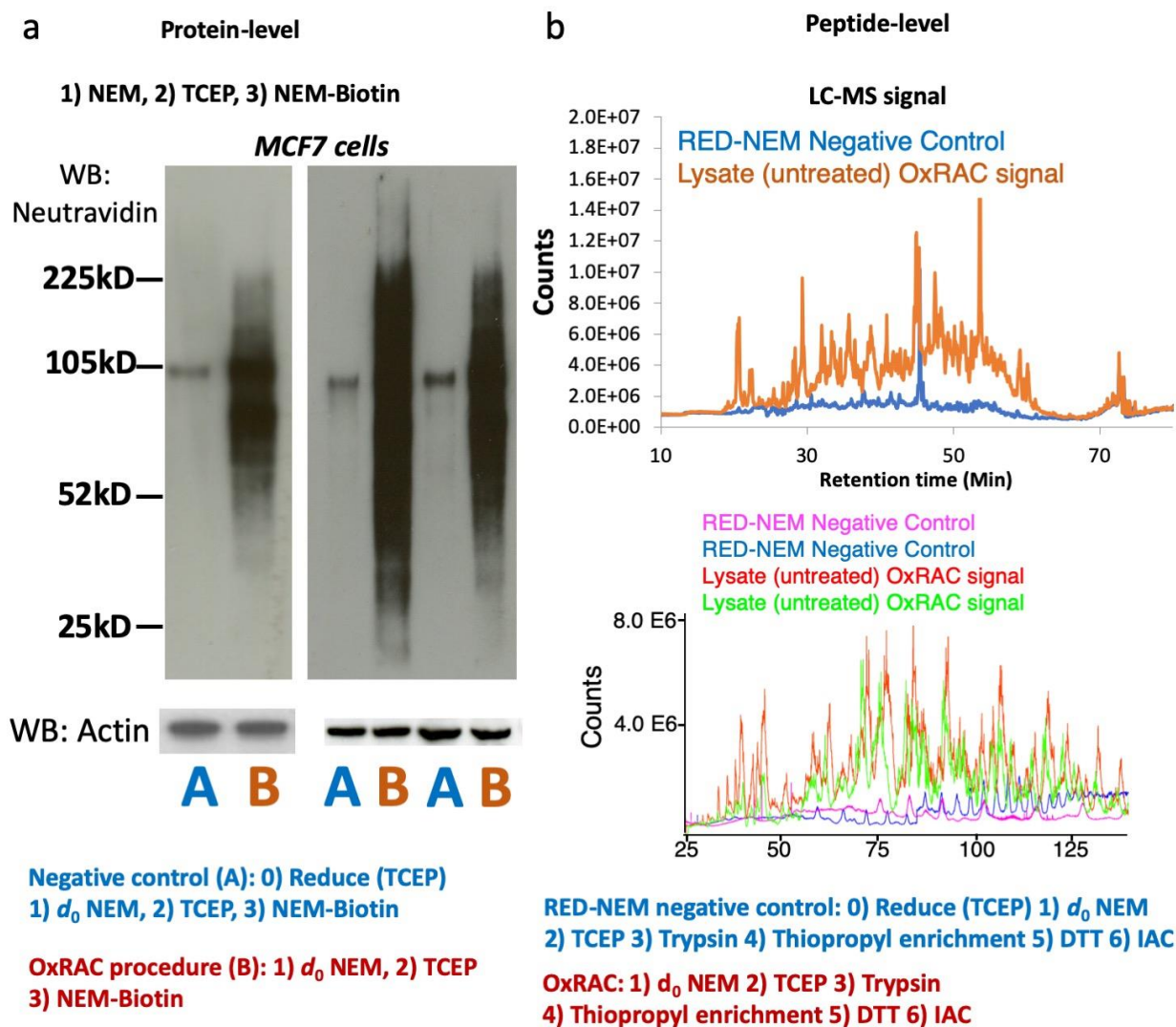
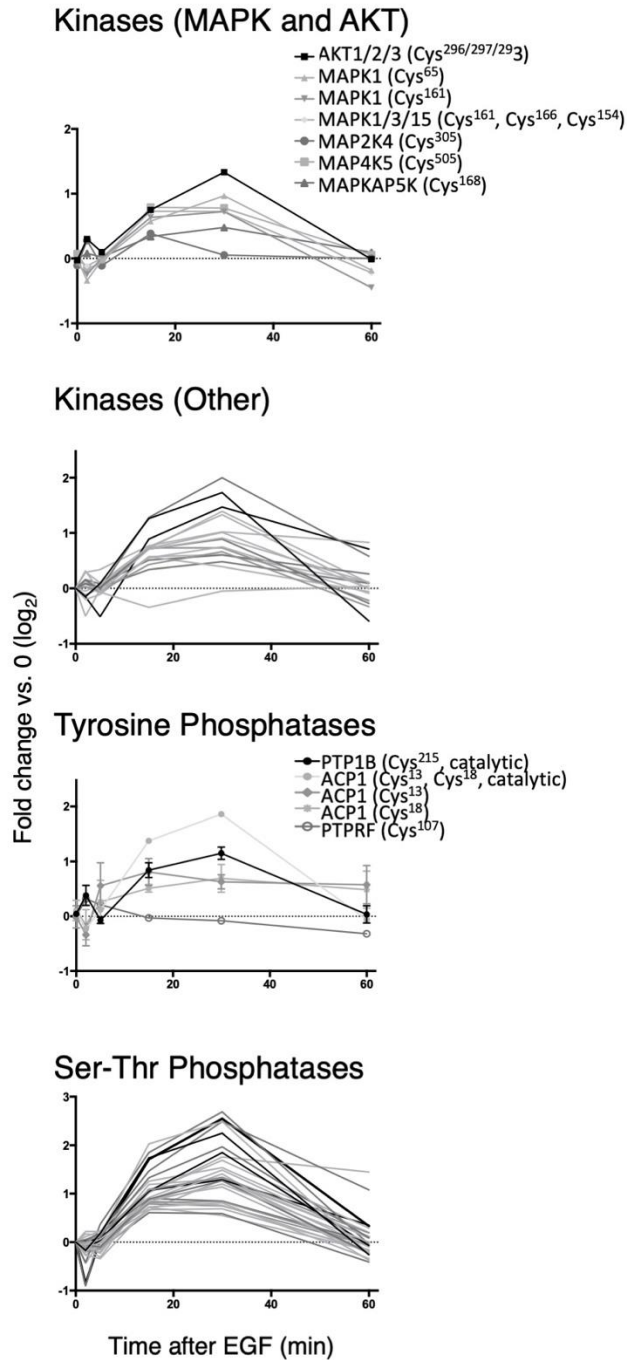


**Fig. S2. OxRAC method validation and controls.** **A)** MCF7 cells were lysed in SDS supplemented with unlabeled NEM as in the OxRAC procedure to block free thiols. After reduction, labeling of previously oxidized cysteine residues with NEM-biotin generates significant signal when blots are probed with neutravidin-HRP. The negative control which is pre-reduced prior to NEM treatment has negligible signal. **B)** Similar experimental design as in A, but with thiopropyl sepharose enrichment and mass spectrometry. 'RED-NEM' samples which are reduced prior to NEM alkylation have very low total ion chromatogram by mass spectrometry and few cysteine-containing peptides identified compared to samples processed for OxRAC analysis.



6

**Fig. S3. Redox regulation of protein kinases and phosphatases.** Time course of redox regulation of cysteine residues in significantly oxidized peptides assigned to kinases and phosphatases. Each line represents one peptide.

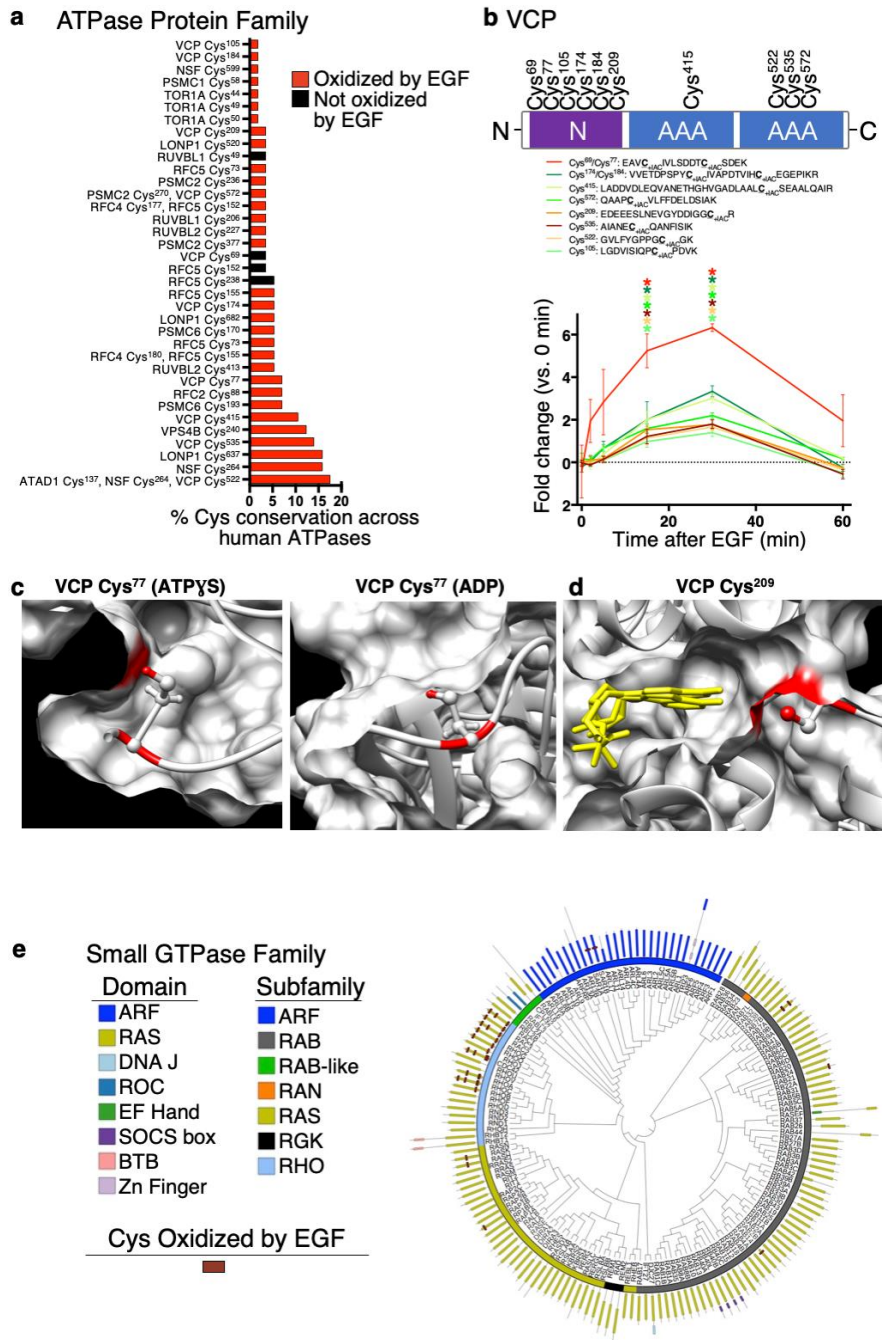


**Fig. S4. EGF-dependent redox regulation of AAA ATPases and small GTPases.** **A)** Amino acid sequence conservation of the cysteine residues identified in AAA ATPase proteins with significant ( $q \leq 0.05$ ,  $N = 3$ ) oxidation by EGF indicated. **B)** Time-dependent changes in the oxidation of all cysteine residues in VCP. Asterisks indicate significance by ANOVA ( $*P < 0.05$ ,  $**P < 0.01$ , based one-way ANOVA with Dunnett's post-hoc test and error bars are SEM for  $N=3$  independent biological replicates). **C)** Crystal structures of VCP. VCP Cys<sup>77</sup> is solvent accessible in the ATPVS VCP structure (PDBID: 5FTN) but buried and solvent inaccessible in the ADP bound state (PDBID:5FTL). The proton on the thiol is colored red as is its contribution to the protein surface. **D)** VCP Cys<sup>209</sup> (red) lies at the base of the nucleotide (yellow) binding pocket. **E)** Phylogenetic analysis of all human small GTPases with the subfamily (inner ring), domain (outer ring), and location of significantly oxidized cysteine residues indicated. Line length corresponds to the number of amino acids with the N-terminus facing the center.

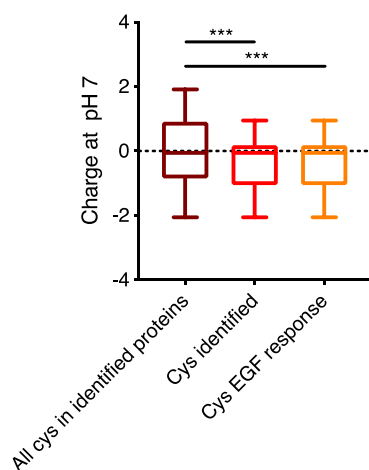


**Fig. S5. Biochemical properties of the identified oxidized cysteine residues.** Net charge at pH 7 for all cysteine residues +/-2 amino acids. Statistical significance was calculated by one-way ANOVA with Tukey's post-hoc test (\*\*\*)  $P < 0.001$ ). Whiskers represent 5 - 95 percentile. N=3 biological replicates.

**Data file S1. Table of all cysteine residues detected, their LC-MS information and intensities, and redox regulation.** The "Site" column indicates the oxidized cysteine residue. Dunnett's multiple comparison test was used to determine statistical significance at each of the 2, 5, 15, 30, and 60 minute time points: 0 represented no statistical significance, 1 represented  $P < 0.05$ , and 2 represented  $P < 0.01$ . The Fuzzy Cluster column indicates the temporal profile: Signal Initiators, SI; Intermediate Stimulators, IS; or Terminal Effectors (TE). RSA: relative solvent accessibility calculated by NetSurfP-2. Secondary structure ( $2^\circ$  Strx): H, helix; C, coil; E, strand.

**Data file S2. PANTHER and Reactome annotations for peptides (and associated genes) assigned to each temporal cluster.**

**Data file S3. IPA canonical pathways enriched at each time point.** Values are  $-\log(p\text{-value})$  calculated by IPA using Fisher's exact test.

**Data file S4. Representation of Pfam domain and family annotations within the OxRAC dataset.** Values are calculated from a two-sided Fisher's exact test comparing domains identified in our dataset to all cysteine-containing domains in the human proteome. †: (-) is under-represented. (+) is over-represented.